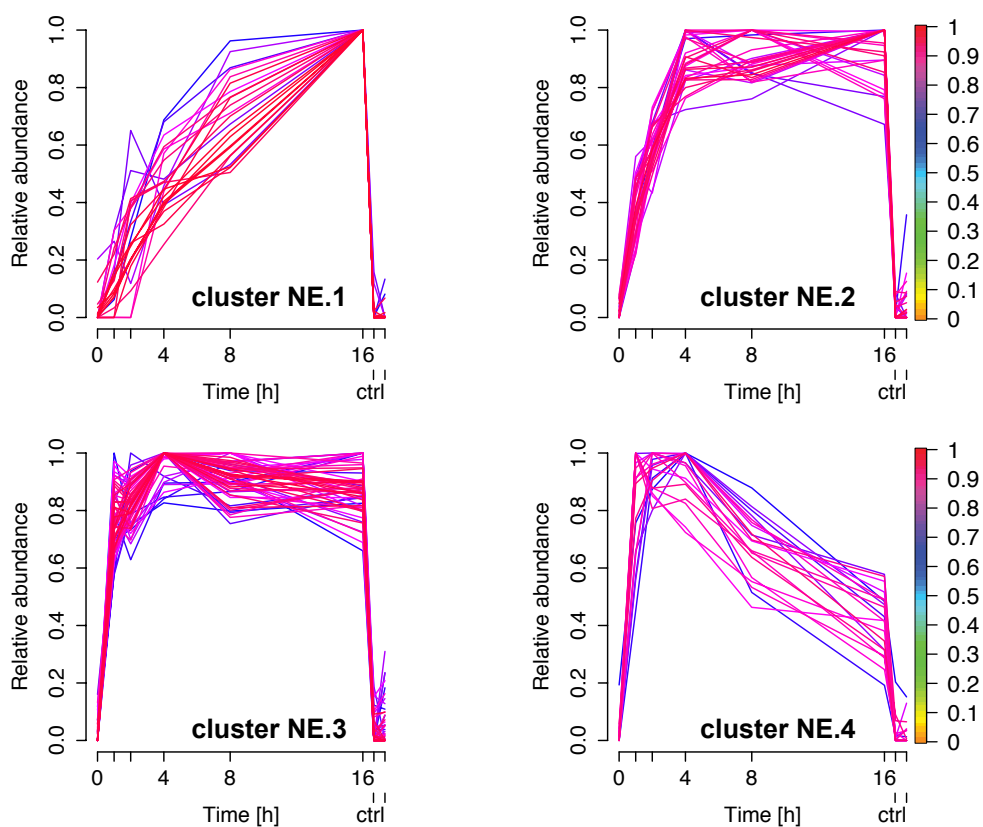


**Figure S1** Determination of catalytic efficiencies for GluC cleavages monitored by 8plex-iTRAQ-TAILS. Data from sub-clusters in Figure 2A were fitted to the well-established pseudo-first-order kinetic equation  $A/A_0 = 1 - e^{-(k_{cat}/K_m * E_0 * t)}$  with  $A/A_0$ : relative abundance and  $E_0$ : enzyme concentration. Cleavages in sub-cluster N.1.2 were considered in a measurable range, and apparent  $k_{cat}/K_m$  values were determined using the equation  $k_{cat}/K_m = \ln 2 / E_0 * t_{1/2}$ , where  $t_{1/2}$  is the time point at which the relative abundance of a neo-N-terminal peptide reaches half of the maximum abundance.



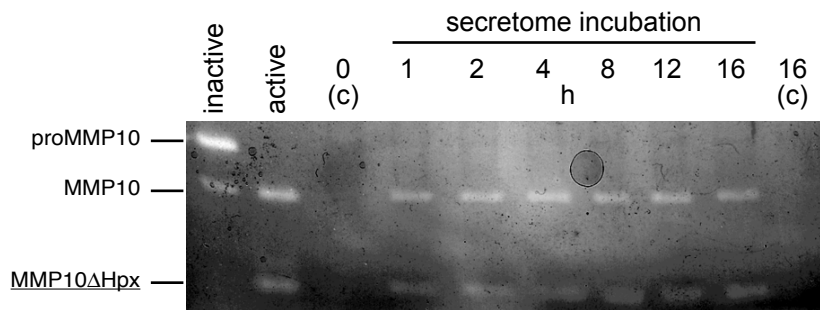
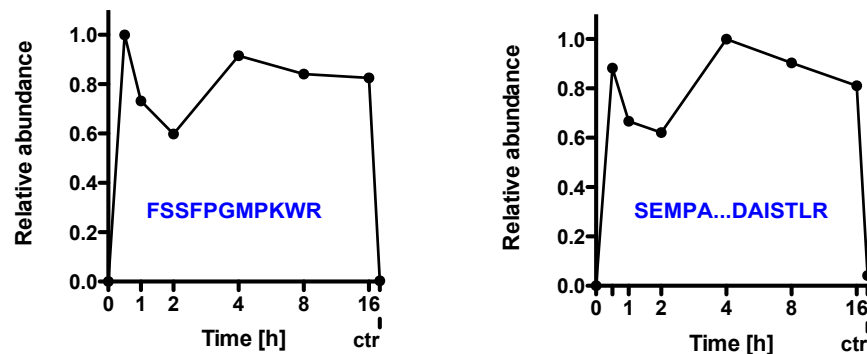
**Figure S2** Fuzzy c means clustering of GluC-generated neo-N termini harboring a single E or D in their sequence. Peptides in clusters NE.1 to NE.3 are either not or to a low extent affected by secondary cleavage, while neo-N termini in cluster NE.4 decrease in abundance upon rapid increase at 2 to 4 hours of incubation. Colorkey indicates membership value  $\alpha$ . For sub-dataset see Supplementary Table S6. ctrl:12 h and 16 h controls.

**A****MMP10\_human (P09238)**

signal peptide

propeptide

MMHLAFLVLLCLPVCSA<sup>YPLSGAAKEEDSNKD</sup>LAQQYLEKY<sup>NLEKDV</sup>KQFR  
 RKDSNLI<sup>VKKIQGMQKFLGLEVTGKLD</sup>TDTLEVMR<sup>KPRCGVPDV</sup>GH<sup>FSS</sup>FPG  
MPKWRKTHLTYRIVNYTPDLPRDAVDSAI<sup>E</sup>KALKVWEEVTPLTFSRLYE<sup>G</sup>E  
 DIMISFAVKEHGDFYSFDGPGHSLAHAYPPGPGLYGDIHFDDDEKWTEDASG  
 TNLFLVAAHELGHSLGLFHSANTEALMYPL<sup>YNSFTE</sup>LAQFRLSQDDVNGIQS  
 LYGPPASTEELVPTKSVPSG<sup>SEMPAKCDPALS</sup>FDAISTLRGEYLF<sup>FFKDR</sup>Y  
 FWR<sup>R</sup>SHWNPEPEFHLISAFWPSLPSYLDAA<sup>YEVNSRDTVFI</sup>FKGNEFWAIRG  
 NEVQAGYPRGIHTLGFPTIRKIDAAVSDKEK<sup>K</sup>KTYFFAADKYWRF<sup>D</sup>ENSQS  
 MEQGF<sup>PRLIADDFPGVEPKVDAVLQAF</sup>GFFYFFSGSSQFEFDPNARMVTHIL  
 KNSWLHC

**B****C**

**Figure S3** Activation and stability of recombinant human MMP10. **(A)** Amino acid sequence of human proMMP10. N-terminal peptides identified by 8plex-iTRAQ-TAILS are indicated in blue. The sequence of an additional autolytic fragment (MMP10 $\Delta$ Hpx) generated upon activation is underlined. Identified neo-N termini resulting from removal of the propeptide and partial autolysis perfectly match with a previous report from Nakamura et al. (1). **(B)** Casein zymography of recombinant human MMP10 before and after auto-activation and samples used for 8plex-iTRAQ-TAILS analysis. Bands correspond to molecular weights of proMMP10, MMP10 and MMP10 $\Delta$ Hpx. Both fragments generated upon auto-activation are stable over the entire time of incubation. **(C)** Kinetic abundance profiles of MMP10 N termini identified by 8plex-iTRAQ-TAILS. Time-dependent differences in abundance for both peptides are within the range of non-cleavage events (Figure 4C) validating the results from zymography. ctrl: 16 h control.

1. Nakamura, H., Fujii, Y., Ohuchi, E., Yamamoto, E., and Okada, Y. (1998) Activation of the precursor of human stromelysin 2 and its interactions with other matrix metalloproteinases. *Eur J Biochem* 253, 67-75

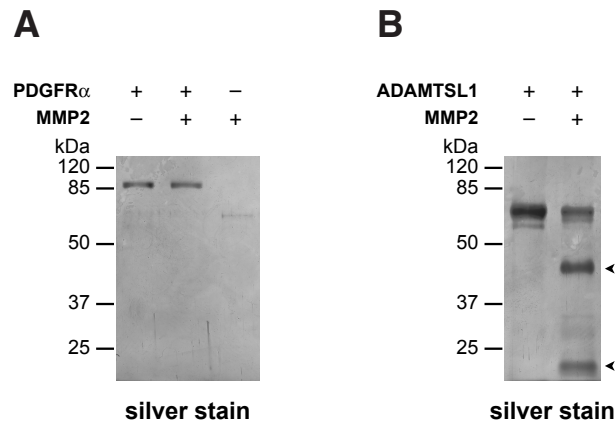


**Figure S4** Processing of PDGFR $\alpha$  and ADAMTSL1 by MMP2. **(A)** Recombinant human PDGFR $\alpha$  (residues 24-524) was incubated with active human MMP2 at 37°C for 16 hours. Proteins were analyzed by SDS-PAGE and silver staining. Lack of processing by MMP2 indicates cleavage by a third activated protease other than MMP10 and MMP2 in MMP10-treated fibroblast supernatants. **(B)** Recombinant human ADAMTSL1 (isoform 1; residues 1-525) was incubated with active human MMP2, and cleavage was monitored by SDS-PAGE and silver staining. Arrows indicate cleavage fragments with equal molecular weights as generated by incubation with MMP10 (Figure 6B), suggesting concomitant activity of both proteases towards ADAMTSL1.